QUASI-POTENTIAL FIELD: THE SIMULATION OF MOTIVATION IN COMPLEX PHYSICAL STRUCTURES

Yang Tian

Department of Psychology
Tsinghua Univesity
Haidian, Beijing, China
tianyang16@mails.tsinghua.edu.cn

Weihua He

Department of Precision Instrument
Tsinghua Univesity
Haidian, Beijing, China
hewh16@mails.tsinghua.edu.cn

Yihan Jia

Department of Engineering Physics
Tsinghua Univesity
Haidian, Beijing, China
jiayh16@mails.tsinghua.edu.cn

ABSTRACT

As a basic element of organisms, motivation shapes the action pattern. There are abundant biological and social systems that originate from motivations, which have attracted widespread attention. To pave the foundation of relevant researches, this paper presents an effective model to simulate the spatial distribution of motivation within complex environments, which is named as the quasi-potential field. Our modelling process includes three steps. First, we suggest an original algorithm for structure reduction, which can preserve all the topological properties of a given environment. Second, we define the quasi-potential value on the reduced structure, which works as the root of the whole field. Third, we extend the field from the root to all the available spaces. Thus, the motivation distribution in the real environment can be finally generated. In our paper, several simulation experiments are carried out to verify the effectiveness of our model, whose results are proved to be ideal.

Keywords: Motivation, Quasi-potential Field, Motivated System.

1 INTRODUCTION

Motivation is the object-dependent tendency of (1) agents, such as human (Atkinson 1964) and other kinds of selected intelligence (Sendhoff, Körner, Sporns, Ritter, and Doya 2009), and (2) unconscious creatures, such as neurons (Lidov, Byers, Watkins, and Kunkel 1990) and leukocytes (Rambeaud, Almeida, Pighetti, and Oliver 2003). For subjects, it describes the trend to approach specific targets during the interaction with environments. As an ubiquitous element in psychology, biophysics and sociophysics, motivation has become the basis of many theories.

On a macro scale, motivation is one of the core parameters for describing the dynamics of biological communities. Previous researches mainly focused on modeling the dynamics induced by specific motivations, which indicated the explicit effects of them. For instance, with the motivation of avoiding predators, prey-flocks show complex variation in the compression and expansion processing of the prey-flock size, which could be simulated by the molecular dynamics in a two-dimensional continuum model (Lee, Pak, and Chon 2006). However, while analysing the mechanisms resulted from motivations clearly, existing studies didn't take the strict, quantitative definitions of motivations into consideration.

On an individual scale, motivation shapes the survival, reproduction and decision-making process. In cognition science, the role of internal motivation in the decision-making process has been explored at both the behavioural level (Kuhl 1986, Finn 2002) and the neutral level (Satoh, Nakai, Sato, and Kimura 2003). It was suggested that lateral intraparietal neurons are sensitive to the motivational salience of cues, which paves the basis for motivation formation and maintain of monkeys (Leathers and Olson 2012). As for human, a lot of researches found that attention and motivations have been confounded and eventually results in distributed signals relevant with them in human brains (Maunsell 2004). The researches in this field went deeply into the biological foundation of motivation, but the labile and complex pattern behind the motivation limited the mathematical modelling.

On the micro scale, motivation defines the formation, migration and patterning of cells and other soft matters. Regulated by different chemicals, cells or molecules are encoded with different functions. Those chemicals works as motivations and shape the pattern of how those cells or molecules form the whole system. Based on neuroscience, it has been confirmed that with different concentrations of signal molecules, there will be patterning in the dorsal ectoderm of chordates, which finally determines all neural tissues (Kandel, Schwartz, Jessell, of Biochemistry, Jessell, Siegelbaum, and Hudspeth 2000). To simulate those properties, a growing number of computational models have been established from the perspective of network dynamics versus topology (Massobrio and Martinoia 2008), statistical fluctuation (Ishii, Ishikawa, Fujita, and Nakazawa 2004) and so on. Using them, we can analysis the dynamics induced by motivations phenomenologically.

To sum up, we can draw a conclusion that on different scales, previous researches have explored the mechanisms behind motivations and the dynamical phenomenons shaped by them. However, it still reminds controversial how to simulate motivations directly. To address this valuable question, we start a new research.

The main ideas, which are also the main contributions, of our research are as following:

- Simulate motivations based on their spatial distributions within physical spaces. The quantitative variation of the objection-dependent tendency can help to define the corresponding field of it, which is called quasi-potential field;
- Treat the physical structure of environment as a basic element of the definition of quasi-potential field, which makes it possible to simulate motivations in real structures, not just in the ideal plane;
- Analyse the interaction between different motivations by doing weighting summation of different quasi-potential fields, which paves the basis of multi-motivations system simulation.

2 BACKGROUNDS AND MATHEMATICAL BASES

To make the details of our new model clear, it's necessary to review its theoretical and technical background. Since the core of our idea is generating the spatial distribution of motivation in the real physical structure, the main problems will be

- how to abstract and represent the physical structure;

- how to measure the spatial variations of motivations in real structures;

As for the physical structure representation, it's unnecessary to load all the details of environment into our method, or the model definition would be expanded to be lots of functions with millions of parameters. To make the model computable, an abstraction method that can keep the topological invariance during the simplification process is required.

As for the measurement of the spatial variations of motivations, we suggest to treat the motivation as a kind of latent variable and use the degree of how individuals are willing to approach the target to represent it. To realize this, we need to know the mechanisms of target approaching under different conditions.

To meet those requirements, several relevant theories and techniques need to be reviewed in detail.

2.1 Topological Structure Abstraction

Homeomorphisms are the mappings that preserve all the topological properties of a given space. Strictly, for a mapping between two topological spaces $f : X \to Y$, it is a homeomorphism if and only if (1) f is a bijection; (2) f and f^{-1} are continuous (Kelley 2017).

Based on homeomorphism, there is a ideal way to do simplification for a given physical structure P and keep the topological invariance, whose result $\widehat{P}$ is defined as

$$\widehat{P} = \bigcap_{i=1}^{\infty} \lambda_i (P), \tag{1}$$

where $\Lambda = \{\lambda_i\}_{i \in I}$ satisfies

- For each $i \in I$, the mapping $\lambda_i : P \to P_i$ is a homeomorphism, and there is $P_i \subset P$;
- For each $i, j \in I$, if $i < j$, then there is $\lambda_j (P) \subset \lambda_i (P)$.

It's clear that for the structure P, this mathematical method can generate a minimum homeomorphic subspace $\widehat{P}$, which is much simpler and topologically equivalent to it. In this paper, $\widehat{P}$ is called the structure root of P.

To realize this method in computers, the set of homeomorphism mappings Λ must be finite. Under this condition, the optimization question of the algorithm can be addressed by (1) defining a set of proper homeomorphism mappings to increase the convergence rate; (2) increasing the number of interaction $|\Lambda|$.

Based on those analyses, we have found a direction to design our original algorithm to abstract the structure root for a given physical structure.

2.2 Target Approaching

There are a lot of functions used for specific goal-gradient description on different scales (Hull 1932, Hull 1938, Bruce 1937). It has been suggested that the gradient of target approaching willing will vary across different motivations (Drew 1939).

On the macro and individual scales, the classic goal-gradient hypothesis posited that the willing to reach a target increases monotonically with proximity to it (Hull 1932). On the micro scale, situations will be

much more complex. Driven by different pheromones or micro-flows, soft matters will show variable target approaching patterns (Stange 1996, Olberg 1983). Recent works mentioned about the individual-based decision algorithm, taking the three-layer model (Handel 2016) and cellular automaton decision rules (Syed and Kunwar 2014) as examples. Those works demonstrate their ability to outperform traditional algorithms such as A*. However, when it comes to a large number of individuals, the individual-based decision algorithms perform poorly due to limited computing capabililty. Structure-based target approaching algorithm could be more capable in this situation.

To simulate those properties on the physical structure P, the ideal way is define a proper mapping $\xi : P_L \to \mathbb{R}$, where

$$P_L = \{\overline{p} \mid \forall (x_i, y_i, z_i), (x_j, y_j, z_j) \in P, \overline{p} = \| (x_i, y_i, z_i) - (x_j, y_j, z_j) \|_L\}, \tag{2}$$

and L is any kind of norm.

The strict definition of ξ can be abstracted from relevant theories based on the specific demands. Using it, we can bridge the gap between the distance space P_L and the motivation value.

3 ALGORITHM MODELLING

Up to now, basic elements that can help to generate the spatial distribution of motivation in the real physical structure have been discovered. Based on them, our original model can be finally established.

In this paper, we will generate the object distribution following those steps:

- First, generate the structure root of a given physical structure, which preserve all its topological properties;
- Second, define the quasi-potential field on the structure root, which is also the root of the whole spatial distribution of motivation;
- Third, generalize the quasi-potential field on the structure root into all the available space of the physical structure, thus the spatial distribution of motivation on the physical structure is finally defined.

Since the real physical structure is usually encode as image data, in this paper, all the arithmetic implementations aim at processing this kind of data. Thus, the norm L used to define metric on the physical structure is defined as the Manhattan distance. Apart of that, to keep the generality, the mapping $\xi : \mathbb{R} \to \mathbb{R}$ is defined as

$$\forall r \in \mathbb{R}, \ \xi(r) = r. \tag{3}$$

3.1 Framework

To make our work easy to understand, here we explain it step by step. At first, the structure root is generated. Then, we compute the quasi-potential values on the root, followed by extending them off the root. The following graph can show our paradigm in detail.

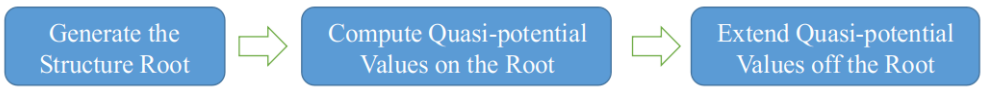

Figure 1: The framework of our approach.

3.2 The Generation of the Structure Root

Serving as the foundation of the quasi-potential field, the structure root reflects the whole structure and provide an overall guidance. For the physical structure P encoded as image data, the main steps to generate it are:

- Binarize the structure according to its availability, which can generate the boundary of it;
- Do morphological erosion for the boundary, which can realize space reduction and keep the topological invariance.

In detail, the algorithm we use to abstract the structure root can corrode boundary from all direction, thus the whole structure will compress with same local velocity. By doing so, in each iteration, we can generate a subspace that is approximatively homeomorphic to the space obtained from last iteration In this paper, the iteration won't stop until the new output subspace is just same as the previous one. Since the physical structure is encoded as image data, we assume its corresponding binary matrix is $P = (p_{ij})_{m\times n}$. Then, the definition of our algorithm is showed as following

Algorithm 1 Structure Root Abstraction

Require: P
Ensure: $\widehat{P}$
$l = 1$
while $P^l \neq P^{l-1}$ **do**
  for $i \in \mathbb{Z} \cap [1, m]$ **do**
    for $j \in \mathbb{Z} \cap [1, n]$ **do**
      if $(l < 2) \wedge \left(\sum_{m \in M_{ij}} m \in \mathbb{Z} \cap [2, 6]\right) \wedge (\rho(M_{ij}, \mathrm{mod}(2, l)) = 0) \wedge (\tau(M_{ij}) = 1)$ **then**
        $p_{ij} \leftarrow 0$,
      end if
      if $(l \geq 2) \wedge \left(\sum_{m \in M_{ij}} m \in \mathbb{Z} \cap [2, 6]\right) \wedge (\rho(M_{ij}, \mathrm{mod}(l, 2)) = 0) \wedge (\tau(M_{ij}) = 1)$ **then**
        $p_{ij} \leftarrow 0$,
      end if
    end for
  end for
  $l \leftarrow l + 1$.
end while
$\widehat{P} \leftarrow P^l$.
return $\widehat{P}$, l,

where for each p_{ij} of P, the matrix M_{ij} is defined as

$$M_{ij} = \{p_{xy} \mid x \in \mathbb{Z} \cap [i-1, i+1],\ y \in \mathbb{Z} \cap [j-1, j+1]\}, \tag{4}$$

it's clear that M_{ij} includes p_{ij} and its Moore Neighbourhood (Figure 2 (b)). Then, the mapping $\rho : M_{ij} \times \{0, 1\} \to M_{ij} \times M_{ij} \times M_{ij}$ is defined as

$$\rho(M_{ij}, r) = \sum_{(p_1, p_2, p_3) \in M_{ij}^r} |\prod_{k=1}^{3} p_k|, \tag{5}$$

in which there are two matrices that define the anti-clockwise search direction in the Moore Neighbourhood of p_{ij}. They are respectively defined as

$$M_{ij}^1 = \{\left(p_{i(j+1)}, p_{(i-1)j}, p_{i(j-1)}\right),\ \left(p_{(i-1)j}, p_{i(j-1)}, p_{(i+1)j}\right)\}, \tag{6}$$
$$M_{ij}^0 = \{\left(p_{i(j-1)}, p_{(i+1)j}, p_{i(j+1)}\right),\ \left(p_{(i-1)j}, p_{i(j+1)}, p_{(i+1)j}\right)\}, \tag{7}$$

during the iteration, we will search in M_{ij}^1 for element 0 when the iteration number is odd. And when the number is not odd, we will search in another half part of the Moore Neighbourhood of p_{ij}.

Moreover, the mapping $\tau : M_{ij} \times M_{ij} \to \mathbb{N}$ is defined as

$$\tau(M_{ij}) = \sum_{(p_1,p_2)\in M_{ij}^+} I_{\{(1,0)\}}((p_1,p_2)) + \sum_{(p_1,p_2)\in M_{ij}^-} I_{\{(0,1)\}}((p_1,p_2)), \tag{8}$$

in which I is the characteristic function, and the matrices M_{ij}^+, M_{ij}^- are defined as

$$M_{ij}^+ = \{\left(p_{(i+1)(j+1)}, p_{i(j+1)}\right),\ \left(p_{i(j+1)}, p_{(i-1)(j+1)}\right),\ \left(p_{(i-1)(j+1)}, p_{(i-1)j}\right)\}, \tag{9}$$
$$M_{ij}^- = \{\left(p_{(i-1)(j-1)}, p_{i(j-1)}\right),\ \left(p_{i(j-1)}, p_{(i+1)(j-1)}\right),\ \left(p_{(i+1)(j-1)}, p_{(i+1)j}\right)\}. \tag{10}$$

If $\rho(M_{ij}, r) = 0$ and $\tau(M_{ij}) = 1$, then in the step r of iteration, there must be an element in the Moore Neighbourhood of p_{ij} that belongs to the boundary of P. So we assign p_{ij} as 0 to compress the boundary near it ,which can realize the reduction.

Based on this method, we can load a topologically equivalent and simplified structure $\widehat{P}$ into our model. The root can indicate the topological information of the environment, which paves the basis of quasi-potential field generation. In the Figure 1, there are two examples of structure roots.

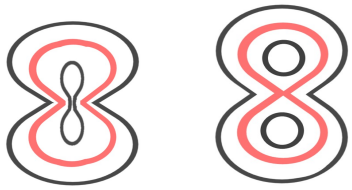

(a) (b)

Figure 2: In (a) and (b), the original structures are marked as black while the structure roots are marked as bold red.

3.3 The Quasi-potential on the Root

After obtaining the structure root, the environment has been corroded into a topologically equivalent structure. To generate the corresponding spatial distributions of motivations in the environment, the first step is to encode the degree of target approaching willing on its root.

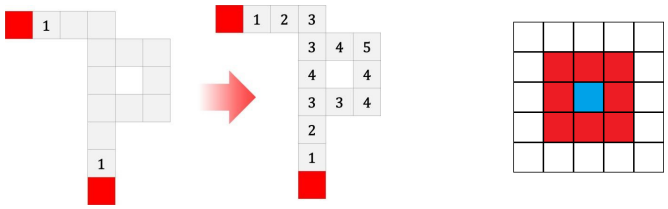

(a) (b)

Figure 3: (a) The quasi-potential on the root. (b) Moore Neighbourhood of the blue cell.

The grey cells in Figure 3 (a) represents the structure root of accessible region. The red cells are the intersections of root and red stairwell regions, defined as destinations.

To obtain the result showed above, we need do the following steps

- Assign the quasi-potential value of the on-root cells adjacent to the destination cells as 1;
- Then, the value of its Moore neighbourhoods (Figure 3 (b)), if on the root, will be higher by 1;
- Move the assignment process that is from each destination step by step and at the same pace. After a designed number of rounds, every cell on root will be assigned a quasi-potential value.

3.4 The Quasi-potential off the Root

On the basis of quasi-potential values of cells on the root, the method of calculation quasi-potential values of the cells off the root needs to be defined.

Our goal is to calculate the quasi-potential value of the blue cell (Figure 4). In each iteration i, we generate a Moore-shape search frame N_i of $4 \times i$ cells, then

- Each cell in the search frame is i-cell-Manhattan-distance from the blue cell;
- If N_i does not cover a cell on the root, in the second iteration we generate N_{i+1} of $4 \times (i+1)$ cells, in which each cell is $i+1$-cell-Manhattan-distance from the blue cell.

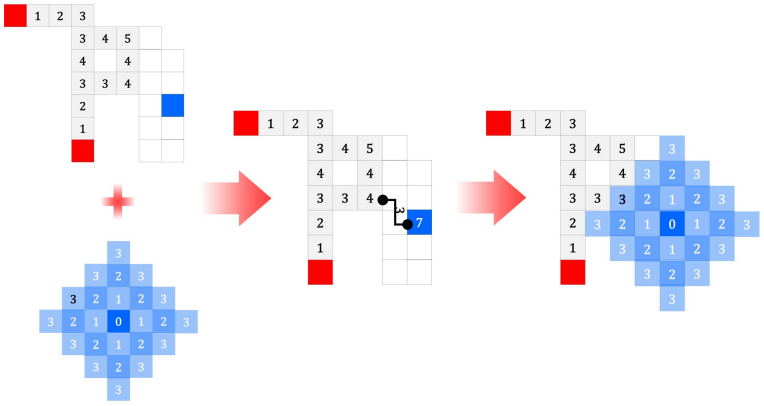

Figure 4: The quasi-potential value of cells off the root.

Mathematically, the quasi-potential value of the blue cell is strictly defined as

$$\phi\left(x_{goal}, y_{goal}\right) = \phi\left(x_{root}, y_{root}\right) + d_M\left(\left(x_{goal}, y_{goal}\right), \left(x_{root}, y_{root}\right)\right), \tag{11}$$

where

- $\phi\left(x_{root}, y_{root}\right)$ is the quasi-potential value of the retrieved root cell, which is defined as

$$\left(x_{root}, y_{root}\right) = \underset{x,y}{\operatorname{argmin}}\, d_M\left(\left(x_{root}, y_{root}\right), (x, y)\right) \tag{12}$$

- $\phi\left(x_{goal}, y_{goal}\right)$ is the quasi-potential value of the goal cell;
- d_M is the Manhattan distance from the goal cell to the retrieved root cell. It is worked out following

$$d_M\left(\left(x_{goal}, y_{goal}\right), \left(x_{root}, y_{root}\right)\right) = \left|x_{goal} - x_{root}\right| + \left|y_{goal} - y_{root}\right| \tag{13}$$

Based on the interaction mentioned above, we can generalize the quasi-potential field on the structure root into the whole space, which works as the spatial distribution of motivation Φ on the original physical structure P.

4 EXPERIMENTS

To verify the effectiveness of our methods, we take the Louvre Museum, whose physical structure is really complex, as an example. The Louvre Museum is known to be a tourist attraction with intense pressure of emergency evacuation. In our experiments, the quasi-potential field of evacuation motivation is generated, which provides abundant information for the security evaluation. Then, a demonstration of the cellular automation based on this quasi-potential field is created to simulate the evaluation of crowds in the Louvre Museum.

4.1 The Structure Root Generation for Complex Construction

The first step of our experiments is abstracting the structure root. Taking the underground floor of the Louvre Museum as an instance, Figure 5 illustrates the modelling procedure of its corresponding structure root.

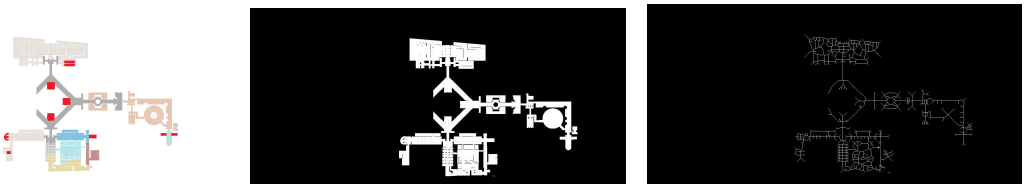

(a) (b) (c)

Figure 5: The map of the floor is pretreated as (a), where the exits of the structure are marked as red. In (b), there is the result after the binarization, in which the available space is transferred into white area while the unavailable space is black. Then the morphological erosion is applied to the white area, leading to the structure root shown in (c).

4.2 The Spatial Distribution of Motivation

Start from the structure root, we assign the quasi-potential value to every cell in the space, thus the whole spatial distribution of motivation can be generated. The gradient maps of two real parts within one floor of Louvre are shown in Figure 6.

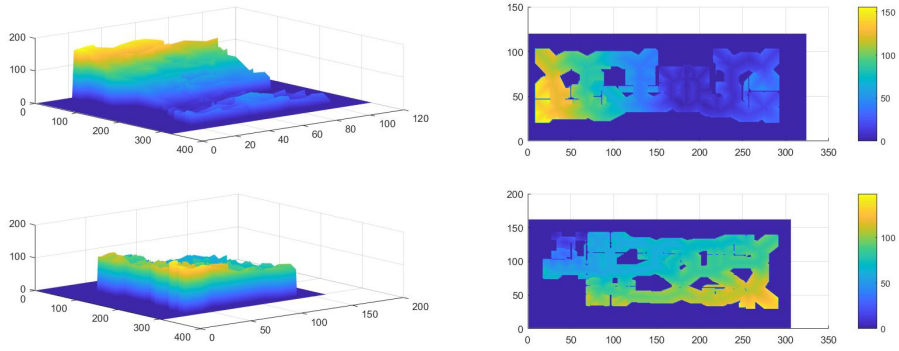

Figure 6: The gradient map of two real parts within the same floor of Louvre.

In these gradient maps, blue region indicates the low quasi-potential value while the red one indicates the high value. For people in Louvre, high quasi-potential means evacuees in these regions are far from known exits, which adds to their difficulty of escaping.

After that, we also generate the corresponding quasi-potential fields of four floors, which are showed in Figure 7.

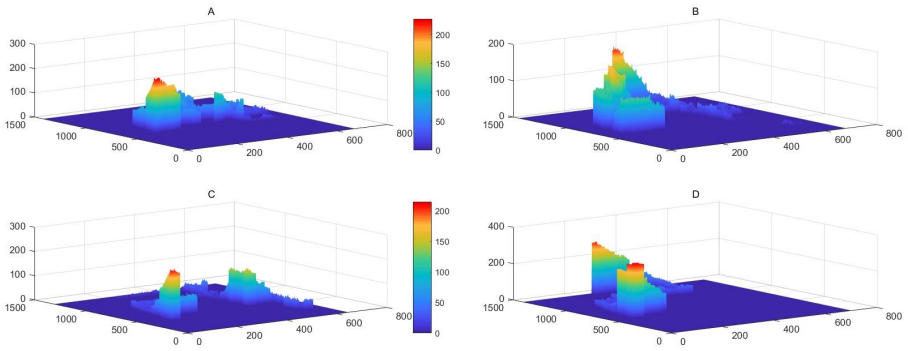

Figure 7: The quasi-potential fields of four floors. A is the first underground floor, B is the ground floor, C is the first floor and D is the second floor.

4.3 Strategy Analyses Based on the Generated Quasi-potential Field

To evaluate the security situation of the Louvre Museum, the simplest way is to find the possible bottle necks during the emergency evacuation.

We can define a function $\beta : \mathbb{R}^2 \to [0, +\infty)$ to find those bottle necks, which is

$$\beta(x,y) = \frac{\phi(x,y)}{|\nabla\phi(x,y)|}, \tag{14}$$

based on this function, we can take both the motivation gradient and the distance between crowds and escape exits into consideration. If $\beta(x,y) \to +\infty$, then it might be necessary to build a new emergency exit at (x,y) since it is a bottle neck.

By calculating, we can generate the following distributions of four different floors, which are showed in Figure 8.

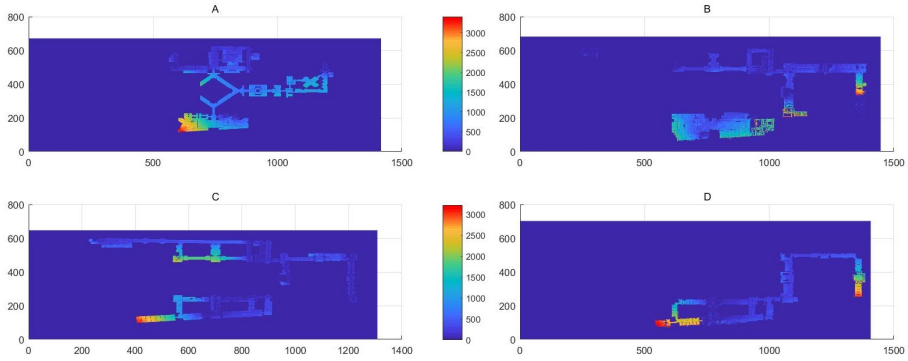

Figure 8: The β distributions of four floors. A is the first underground floor, B is the ground floor, C is the first floor and D is the second floor.

In those graphs, the points marked as red or orange are the bottle necks during the emergency evacuation. To improve the security situation of the Louvre Museum, new contingency strategies or means of escape should be designed for those places.

4.4 Demonstration of the Cellular Automation based on the Quasi-potential Field

Finally, we demonstrate a simple cellular automation based on our quasi-potential field in order to visualize the evacuation model.

The settings of this experiment are as following

- People in the structure are represented by blue points;
- For every step of the cellular automation, each point would choose the point with the lowest quasi-potential field in the surrounding points to move;
- If there are multiple points with the same quasi-potential value on the surrounding points, then randomly select one from them;
- In addition, if every point around has a higher quasi-potential value than itself, then the blue point would stay in place;
- When two blue points try to move to the same location, randomly pick one from them and the other one should re-plan its action.

There are 100 people in total, they need to do evacuation in a real region of the Louvre Museum. The following graphs indicate their situation sequence:

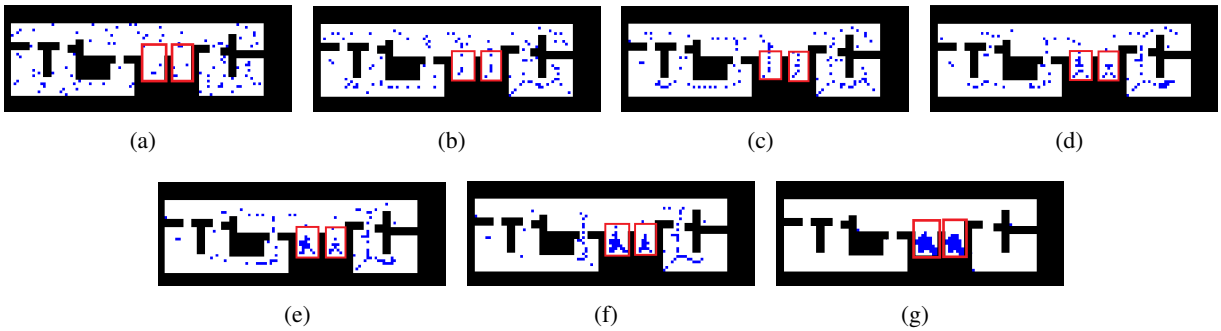

(a) (b) (c) (d)

(e) (f) (g)

Figure 9: The targets of crowds are two exits marked by red box. From (a) to (g), the graphs respectively show the situation of the initial, 4th, 8th, 20th, 40th, 70th and final steps of the iteration. In the last graph, it can be seen that all the individuals have finished their evacuation successfully.

5 DISCUSSION

We have proposed a novel quasi-potential field, which can simulate the motivation distribution in any physical structure. Using the topological properties of the given environment, the calculation complexity of quasi-potential field has been reduced significantly, which enables it to adapt to complex situations. Based on experiment results, our model has been proved to be a promising approach to analyzing the motivated system. In the future work, we will deploy the quasi-potential field in various scenes. For instance, simulating the growth of neural system on a micro scale via the quasi-potential field will be a valuable direction, which can contribute to neuroscience. To sum up, the quasi-potential field is an effective model for motivation simulation, based on which, abundant new researches can be carried out.

REFERENCES

Atkinson, J. W. 1964. “An introduction to motivation.”.

Bruce, R. H. 1937. “An experimental investigation of the thirst drive in rats with especial reference to the goal gradient hypothesis”. *The Journal of General Psychology* vol. 17 (1), pp. 49–62.

Drew, G. 1939. “The speed of locomotion gradient and its relation to the goal gradient.”. *Journal of Comparative Psychology* vol. 27 (2), pp. 333.

Finn, P. R. 2002. “Motivation, working memory, and decision making: A cognitive-motivational theory of personality vulnerability to alcoholism”. *Behavioral and Cognitive Neuroscience Reviews* vol. 1 (3), pp. 183–205.

Handel, O. 2016. “Modeling dynamic decision-making of virtual humans”. *Systems* vol. 4 (1), pp. 4.

Hull, C. L. 1932. “The goal-gradient hypothesis and maze learning.”. *Psychological Review* vol. 39 (1), pp. 25.

Hull, C. L. 1938. “The goal-gradient hypothesis applied to some" field-force’problems in the behavior of young children.”. *Psychological Review* vol. 45 (4), pp. 271.

Ishii, D., K. L. Ishikawa, T. Fujita, and M. Nakazawa. 2004. “Stochastic modelling for gradient sensing by chemotactic cells”. *Science and Technology of Advanced Materials* vol. 5 (5-6), pp. 715–718.

Kandel, E. R., J. H. Schwartz, T. M. Jessell, D. of Biochemistry, M. B. T. Jessell, S. Siegelbaum, and A. Hudspeth. 2000. *Principles of neural science*, Volume 4. McGraw-hill New York.

Kelley, J. L. 2017. *General topology*. Courier Dover Publications.

Kuhl, J. 1986. "Motivation and information processing: A new look at decision making, dynamic change, and action control.".

Leathers, M. L., and C. R. Olson. 2012. "In monkeys making value-based decisions, LIP neurons encode cue salience and not action value". *Science* vol. 338 (6103), pp. 132–135.

Lee, S.-H., H. Pak, and T.-S. Chon. 2006. "Dynamics of prey-flock escaping behavior in response to predator's attack". *Journal of theoretical biology* vol. 240 (2), pp. 250–259.

Lidov, H. G., T. J. Byers, S. C. Watkins, and L. M. Kunkel. 1990. "Localization of dystrophin to postsynaptic regions of central nervous system cortical neurons". *Nature* vol. 348 (6303), pp. 725.

Massobrio, P., and S. Martinoia. 2008. "Modelling small-patterned neuronal networks coupled to microelectrode arrays". *Journal of neural engineering* vol. 5 (3), pp. 350.

Maunsell, J. H. 2004. "Neuronal representations of cognitive state: reward or attention?". *Trends in cognitive sciences* vol. 8 (6), pp. 261–265.

Olberg, R. M. 1983. "Pheromone-triggered flip-flopping interneurons in the ventral nerve cord of the silkworm moth, Bombyx mori". *Journal of Comparative Physiology A: Neuroethology, Sensory, Neural, and Behavioral Physiology* vol. 152 (3), pp. 297–307.

Rambeaud, M., R. Almeida, G. Pighetti, and S. Oliver. 2003. "Dynamics of leukocytes and cytokines during experimentally induced Streptococcus uberis mastitis". *Veterinary immunology and immunopathology* vol. 96 (3-4), pp. 193–205.

Satoh, T., S. Nakai, T. Sato, and M. Kimura. 2003. "Correlated coding of motivation and outcome of decision by dopamine neurons". *Journal of neuroscience* vol. 23 (30), pp. 9913–9923.

Sendhoff, B., E. Körner, O. Sporns, H. Ritter, and K. Doya. 2009. *Creating brain-like intelligence: from basic principles to complex intelligent systems*, Volume 5436. Springer.

Stange, G. 1996. "Sensory and behavioural responses of terrestrial invertebrates to biogenic carbon dioxide gradients". In *Advances in Bioclimatology_4*, pp. 223–253. Springer.

Syed, U. A., and F. Kunwar. 2014. "Cellular automata based real-time path-planning for mobile robots". *International Journal of Advanced Robotic Systems* vol. 11 (7), pp. 93.

AUTHOR BIOGRAPHIES

YANG TIAN is an undergraduate student of the Department of Psychology at Tsinghua University. He is a member of the Cognition Neuroscience Lab, whose research interests include brain-like intelligence, computational neuroscience, biophysics and neural engineering. His email address is tianyang16@mails.tsinghua.edu.cn.

WEIHUA HE is an undergraduate at the Department of Precision Instruments , Tsinghua University, Beijing. Weihua does research in mechanical engineering, microfluidic engineering and signal processing. His email address is hewh16@mails.tsinghua.edu.cn.

YIHAN JIA is an undergraduate of the Department of Engineering Physics in Tsinghua University, China. Her research interests include simulation modeling, health physics and phantom dosimetry. Her email address is jiayh16@mails.tsinghua.edu.cn.